

The emerging role of advanced neuroimaging techniques for brain metastases

Martha Nowosielski^{1,2}, Alexander Radbruch^{2,3}

¹Department of Neurology, Medical University Innsbruck, Innsbruck, Austria; ²Department of Neuroradiology, University of Heidelberg Medical Center, Heidelberg, Germany; ³Department of Radiology, DKFZ, Heidelberg, Germany

Correspondence to: Martha Nowosielski, MD, PhD. Department of Neurology, Medical University Innsbruck, Anichstrasse 35, A-6020 Innsbruck, Austria. Email: Martha.Nowosielski@i-med.ac.at.

Abstract: Brain metastases are an increasingly encountered and frightening manifestation of systemic cancer. More effective therapeutic strategies for the primary tumor are resulting in longer patient survival on the one hand while on the other, better brain tumor detection has resulted from increased availability and development of more precise brain imaging methods. This review focuses on the emerging role of functional neuroimaging techniques; magnetic resonance imaging (MRI) as well as positron emission tomography (PET), in establishing diagnosis, for monitoring treatment response with an emphasis on new targeted as well as immunomodulatory therapies and for predicting prognosis in patients with brain metastases.

Keywords: Brain metastases; functional neuroimaging; magnetic resonance imaging (MRI); positron emission tomography (PET)

Submitted Apr 02, 2015. Accepted for publication May 14, 2015.

doi: 10.3978/j.issn.2304-3865.2015.05.04

View this article at: <http://dx.doi.org/10.3978/j.issn.2304-3865.2015.05.04>

Introduction

Early detection of brain metastases as a result of more precise and innovative neuroimaging modalities as well as improvements in oncology treatments, are leading to longer patient survival (1) but also to an increasing incidence of brain metastases (2-4).

Standard magnetic resonance imaging (MRI) has high detection sensitivity but low specificity in differentiating brain tumors and treatment related changes (5). Contrast enhancement in T1 weighted images basically reflects a disrupted blood brain barrier and T2 signal hyperintensity, is a combination of infiltrating tumor cells, necrotic areas, tumor edema and treatment related leukoencephalopathy. It has been shown that although contrast enhanced MRI is the method of choice to evaluate primary and secondary brain tumors, it is not always capable of providing conclusive data to be able to reliably differentiate tumors from treatment-related imaging findings such as non-specific inflammatory reactions caused by irradiation and chemotherapy ('pseudoprogression') or postoperative enhancement

along the resection margins (6). With the advent of innovative therapeutic strategies, especially anti-angiogenic, targeted and immunogenic therapies, new and even more sophisticated challenges for disease monitoring already have and will continue to develop in the next few years (7-11). As these new therapeutic possibilities become more available, advanced neuroimaging techniques are likely to play a more prominent role in better management of brain metastases.

Advanced neuroimaging techniques

Before discussion of the various fields of application in functional neuroimaging methods, it is important to briefly describe the modalities and their reported parameters. The following imaging modalities will be discussed in this review; diffusion weighted MRI (DW-MRI), perfusion MRI, proton magnetic resonance spectroscopy (MRS) and various ¹⁸F-labelled tracers with the focus on amino acid tracers in positron emission tomography (PET) (Figure 1).

Diffusion Weighted images detect the movement of free water and allow surrogate diffusion to be calculated for

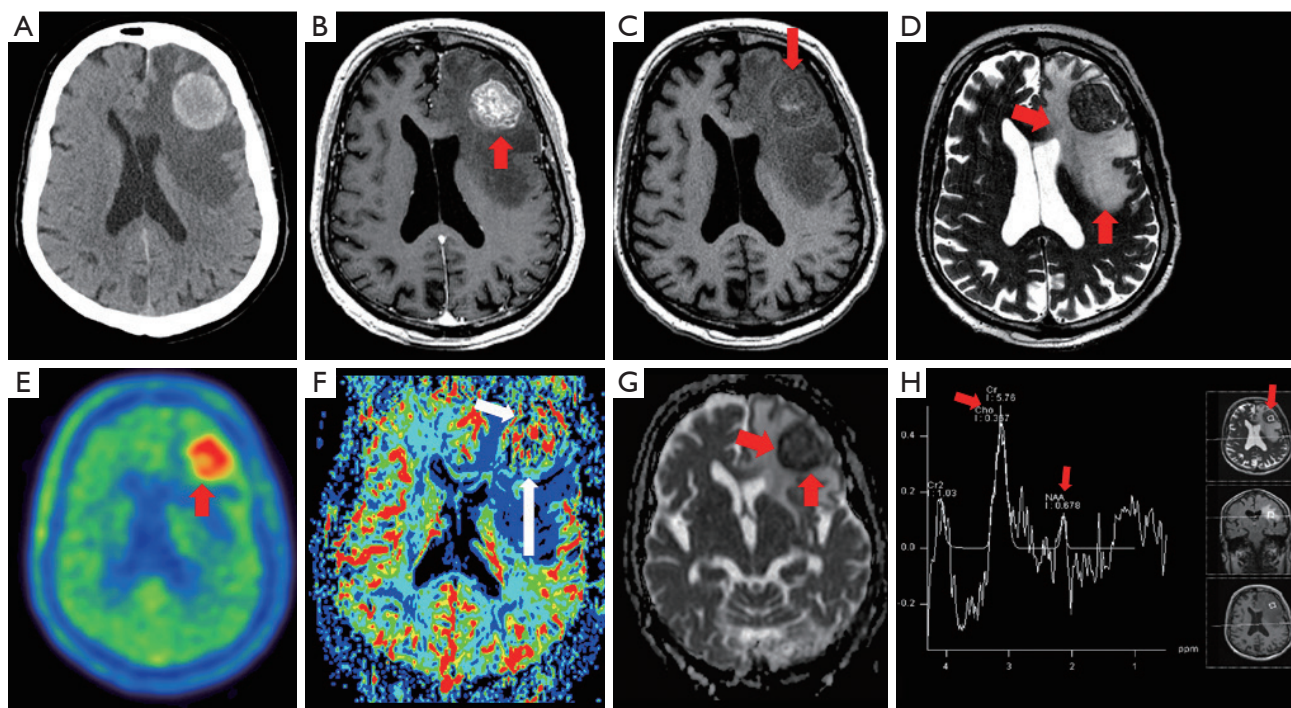


Figure 1 An 81-year-old male patient presents with a first epileptic seizure. An initial native head CT scan (A) shows a left frontal space occupying lesion. MRI, including functional MRI sequences, characterizes the lesion more precisely (B) T1 weighted MRI at 1.5 Tesla with single dose (0.1 mmol/kg) gadolinium contrast delineates an inhomogeneous lesion (C) T1 weighted native scan describes a small bleeding and necrotic areas; (D) T2 weighted MRI shows the lesion with massive peritumoral edema; (E) 18F-FET-PET shows increased tracer uptake; (F) perfusion weighted MRI is able to detect increased cerebral blood volume in the contrast up-taking part of the lesion, not in the peritumoral edema; (G) DW-MRI with ADC measurement shows reduced diffusion at the site of the solid part of the lesion with increased diffusion due to vasogenic edema in the white matter surrounding the mass; (H) MR spectroscopy yields an abnormal spectrum with reduced NAA, reduced Cr and elevated Cho. The patient was referred to surgery and histology revealed squamous epithelium, most probably representing a metastasis from a carcinoma of the esophagus. DW-MRI, diffusion weighted MRI; ADC, apparent diffusion coefficient; NAA, N-acetyl aspartate; Cho, choline.

each voxel to generate apparent diffusion coefficient (ADC) maps. DW-MRI is able to yield ultrastructural information on cellular density and properties of the extracellular matrix (12) and has been linked to lesion aggressiveness and tumor response (13). In a large extracellular volume, which may be caused by fluid accumulation (e.g., tumor edema) the ADC is high.

MR Perfusion may be performed using a variety of methods. Most commonly, perfusion imaging is developed from the administration of gadolinium based contrast while repeatedly sampling signals from brain tissues of interest. This may be performed using or T2* weighted dynamic susceptibility contrast (DSC) or T1 weighted dynamic contrast enhanced (DCE) techniques. A commonly reported perfusion parameter obtained from both DSC

and DCE techniques is the relative cerebral blood volume (CBV). This is calculated by comparing the CBV in the region of interest surrounding the lesion concerned, to the CBV of an identical region of interest surrounding the normal appearing white matter in the contralateral cerebral hemisphere (14-16). Additional parameters may be calculated from perfusion studies, including parameters such as time to peak contrast level, cerebral blood flow and capillary permeability.

MRS allows tissue metabolites to be assessed non-invasively. The two main techniques use single voxel or multivoxel chemical shift imaging techniques. Metabolites commonly evaluated in brain spectroscopy include; choline a marker of cell membrane turnover, N-acetyl aspartate (NAA) a marker of neuronal integrity, lactate a marker of

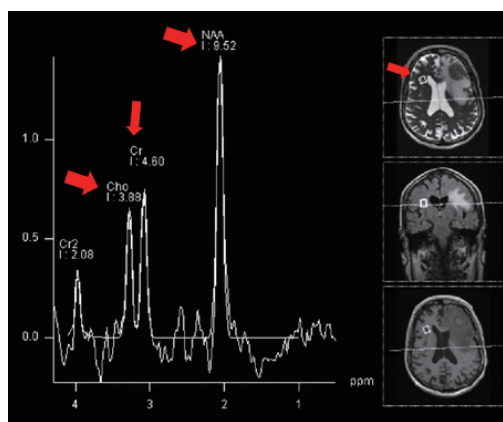


Figure 2 Example for healthy tissue. Metabolites commonly evaluated in brain spectroscopy include; Cho, a marker of cell membrane turnover, NAA, a marker of neuronal integrity. Creatine is often used as an internal control against which other metabolite peaks are compared. Common ratios evaluated in proton spectroscopy of the brain include the choline/creatine ratio and the Cho/NAA ratio. NAA, N-acetyl aspartate; DW-MRI, diffusion weighted MRI; Cho, choline.

anaerobic metabolism and lipid a by-product of necrosis. Creatine is often used as an internal control against which other metabolite peaks are compared. Common ratios evaluated in proton spectroscopy of the brain include the choline/creatine ratio and the choline/NAA ratio (14,17), (Figure 2).

Molecular imaging with PET visualizes metabolic pathways and along with the group of positron-emitting radiolabelled compounds 2-deoxy- ^{18}F fluoro-D-glucose (^{18}F FDG) is the most widely used because it is available in all PET centers (18). The uptake mechanism of ^{18}F FDG in tumor cells depends on the increased number of functional glucose transporters and glycolytic enzymes (18). However, due to a high physiological glucose uptake of ^{18}F FDG in normal brain parenchyma and the low resolution power of PET scans (5 mm), its use is limited in brain tumor detection (19,20). Radiolabeled amino acids are of particular interest for brain tumor imaging (21) because they provide high sensitivity for the detection of primary tumors, recurrent or residual gliomas, including most low grade gliomas (22) and their uptake is high in biologically active tumor tissue but low in normal brain tissue (23). In gliomas ^{18}F -FET uptake significantly correlates with tumor cell density and proliferation rate as well as with microvascular density and neoangiogenesis (24,25).

Diagnosis of brain metastases

Brain metastases may occur in 20-40% of patients with cancer and are symptomatic during lifetime for 60-75% (26). In adults the primary tumors most likely to metastasize in the brain originate from lung (minimum 50%), skin (melanoma 10-40%), breast (15-25%), colon/rectum and kidney cancer (26). Brain metastases are more often diagnosed in patients with known malignancy but up to 30% of brain metastases are diagnosed either at the time of primary tumor diagnosis or before the discovery of the primary tumor.

Is screening therefore indicated? Cerebral MRI is indicated in all patients with established malignant disease if clinical history is strongly suggestive of the presence of brain metastases (26). Current guidelines by the European Society for Medical Oncology (ESMO) recommend screening for brain metastases in patient with carcinoma of the lung with clinical stage III or IV disease even if neurologically asymptomatic or particularly in stage III disease in patients with a curative intent (27). Brain imaging should not be carried out routinely in metastatic breast cancer patients, if the patient is asymptomatic (28) and also for melanoma patients there is currently no consensus on the frequency of follow-up (29). Two recent studies lately challenge these guidelines. O'Dowd *et al.* (30) did a retrospective analysis on 646 patients who underwent surgery for lung cancer with curative intent and identified those who developed brain metastases in the postoperative period. There was a 6.3% incidence of postoperative brain metastases, more commonly in adenocarcinoma and 71% of those who developed cerebral metastases might have been detected in case they had undergone a cerebral MRI as part of their initial staging (4.4% of all patients). The authors concluded that cerebral MRI should be recommended in addition to standard staging investigations and patients should have brain imaging prior to curative surgery in non-small cell lung cancer (NSCLC) regardless of the preoperative stage. Kung *et al.* (31) retrospectively calculated the prevalence of unknown brain metastases detected by FDG PET/CT in 1,876 patients of which 17 patients were diagnosed with primary unknown cerebral metastases. In these patients a change of treatment occurred in 94.1% (16/17 patients).

Headaches (40-50%), focal neurological deficits (30-40%) and seizures (15-20%) are the most common presenting symptoms (26). A minority of patients have an acute stroke-like onset, more often related to an intratumoral hemorrhage (melanoma, choriocarcinoma

and renal carcinoma). Altered mental status or impaired cognition are seen in patients with multiple metastases and/or increased intracranial pressure (26). Contrast-enhanced MRI is more sensitive than enhanced CT (including double-dose delayed contrast) or unenhanced MRI in detecting brain metastases, particularly when located in the posterior fossa (32). Double or triple doses of gadolinium-based contrast agents are better than single doses but increasing the dose may lead to an increased number of false positive findings (33). A peripheral location, spherical shape, ring enhancement with prominent peritumoral edema and multiple lesions all suggest metastatic disease. These characteristics are helpful but not diagnostic, even in patients with a history of cancer.

Differential diagnosis of brain metastases includes malignant gliomas and lymphomas or non-neoplastic conditions, e.g., abscesses, infections, demyelinating diseases, and vascular lesions. At present there are no pathognomonic features on CT or MRI that distinguish brain metastases from primary brain tumors. It has been proposed that mucinous metastases show low T2 signal intensities, and that metastases from melanoma show a high signal on non-contrast T1 imaging. Such signal characteristics, however, can vary substantially and may change over time due to hemorrhages or the accumulation of melanin and paramagnetic ions, e.g., in melanoma (34,35). Through the use of advanced neuroimaging facilities efforts are being made to overcome these problems.

DW-MRI is commonly used for the differential diagnosis of ring-enhancing cerebral lesions. Restricted diffusion is thought to characterize abscesses compared to unrestricted diffusion which is found in cystic or necrotic glioblastomas or metastases. Unfortunately these findings are not specific as restricted diffusion has also been reported in cerebral metastases of certain histological subtypes (breast, colon, testicular, small and NSCLC) (36-39). DW-MRI has also been used to differentiate high grade gliomas (HGG) from metastases but with even more contradictory evidence. The main hypothesis for the evaluation of functional neuroimaging in this setting is that the peritumoral region in primary brain tumors contains vasogenic edema as well as infiltrating tumor cells and angiogenesis, whereas in metastases this area is thought to represent only vasogenic edema, since metastases are more circumscribed. Therefore the peritumoral region in metastases is assumed to show greater diffusion restriction in DW-MRI as well as lower perfusion values in perfusion MRI compared to the peritumoral region in primary brain tumors. In DW-MRI

analysis this hypothesis was proved to be correct in some studies (40,41) but was disproved in others (42,43). It was believed that the wide variations of methodology (post-processing, imaging acquisition and scanner use) was responsible for this contradiction but recently it has been shown that brain metastases may also show an infiltrative phenotype independently from the primary tumor type (44).

The 'peritumoral region' hypothesis was also evaluated by perfusion MRI, where it was shown to be more robust as the peri-tumoral region (45,46) as well as the solid tumor region (47,48) in HGG showed higher CBV values compared to metastases. Recently, by implementing a specific mathematical leakage correction, differences in CBV were also detected between pyogenic brain abscesses, glioblastomas and/or cystic metastatic brain tumors (49). The peritumoral region was also the focus of interest in MR spectroscopy where it was shown that in metastases the Cho/creatinin ratio was lower compared to HGG with excellent sensitivity and specificity (50,51). In nuclear medicine, retrospective analysis (5) of 393 patients failed to show that ^{18}F -FET uptake quantified by static standardized uptake values (SUVs) could differentiate between high grade tumors of glial or non-glial origin, including metastases (HGG, $n=131$; median SUV compared to contralateral hemisphere, $1.99+0.74$) versus high-grade non-glial tumors, $n=25$; median SUV, $2.09+0.62$).

In the future a multiparametric approach will hopefully give the best solution to differentiate primary brain tumors from secondary and non-neoplastic lesions, as it already was shown that perfusion MRI and CBV values in addition to Cho/Cre ratio in MR spectroscopy could differentiate between these two pathologies (46,52).

What is the underlying primary?

Another field of research for functional neuroimaging methods in the field of brain metastases is to add information on the underlying primary tumor, since at the time brain metastases are diagnosed the primary tumor is unknown in up to 10-15% of patients. In this context MR spectroscopy analysis was able to differentiate NSCLC from breast and melanoma metastases by showing a lower Cho/Cre ratio in NSCLC (52). Susceptibility-weighted imaging has also been shown to be very sensitive in detecting melanoma metastases. Approximately 66% of melanoma metastases show intratumoral susceptibility signals which sets them apart from other metastases (e.g., lung and breast cancer show less) with a specificity of approximately

81-96% (53,54).

A recent Chinese study investigated brain metastases from esophageal carcinoma and characterized them on T1-weighted MRI images as having enhanced single or multiple cystic lesions with an edema zone <2 cm in diameter (55). In addition specific radiographic characteristics could be assigned for triple negative breast cancer metastases in another study. Each brain metastasis (n=62) was classified as solid, cystic necrotic, leptomeningeal spread, or mixed type and triple negative brain metastases were shown to be significantly more often cystic necrotic (56).

Treatment planning

New areas for the application of neuroimaging in brain metastases will also include treatment planning. An interesting study by Momose *et al.* (57) investigated the value of amino acid PET (^{11}C -MET) in stereotactic radiotherapy treatment planning for focal recurrence at a previous irradiated site of a brain metastasis. In 88 patients the authors found that the total irradiation volume was significantly smaller in the PET group and that the median survival time was significantly longer in the PET group (18.1 months) than in the MRI planning group (8.6 months, $P=0.01$). Intraoperative neuronavigation could also be an upcoming field of research because, as mentioned above, brain metastases from various tumor types may show differences in the invasion pattern (44). In a small study by Zakaria *et al.* it has been shown that fusing ADC maps with structural scans for intraoperative neuronavigation is a useful method for sampling the border zone of brain metastases (58).

Treatment response

The ability to predict response to treatment may enable early termination of treatment in non-responsive patients, prevent additional toxicity and allow early changes in treatment (59). Unlike new treatment response criteria for solid somatic tumors, Response Evaluation Criteria in Solid Tumors (RECIST), or the updated evaluation criteria for glioma, Response Assessment in Neuro-oncology (RANO), the basis for evaluation of treated brain metastases still remains uncertain (60-62). Since serial tissue biopsies are not practical in brain metastases and in the light of new upcoming targeted treatment, tools to measure drug penetration, pharmacodynamic effects and efficacy become increasingly important.

In a study of lapatinib among patients with HER2-positive breast cancer, reductions in the ^{18}F -FDG uptake in brain metastases were seen in a subset of women, providing some of the first *in vivo* evidence that the drug reaches levels in patients with brain metastases sufficient to influence cellular signaling (63). An alternative PET-based approach has been to develop reagents to non-invasively measure drug uptake in a more direct fashion. Examples include ^{89}Zr -trastuzumab (64) and ^{89}Zr -bevacizumab (65) PET imaging, which have been shown to be feasible in patients with breast cancer.

It is not yet clear how novel targeted therapies (e.g., immunotherapies and kinase inhibitors) will alter imaging characteristics. In gliomas we became aware that anti-angiogenic treatment targeting the VEGF pathway causes a rapid decrease in T1 contrast-enhancing tumor parts with high radiographic response rates ranging between 30% and 63% (66). This decrease was largely due to a “pseudo-normalization” of an abnormal BBB permeability followed by a reduction in tumor edema. Therefore, anti-angiogenic therapy causes difficulties in distinguishing between anti-vascular and true anti-tumor effects (67,68). In patients with glioblastoma, anti-angiogenic treatment response was shown to be more reliably monitored by various functional neuroimaging techniques, including DW-MRI (69,70), perfusion MRI (71,72), ^{18}F -FET-PET (5), MR spectroscopy (73), T2 mapping (74) or T1 subtraction maps (75). Similar studies are ongoing in patients with breast cancer to determine whether early vascular changes in response to anti-angiogenic therapy might be predictive of clinical outcomes (1).

Apart from immune-related side effects, such as hypophysitis (reported in a small percentage of patients during ipilimumab therapy) or granulomatous disease (neurosarcoid) (35), immunoinhibitory therapeutic agents produce anti-tumor effects by inducing cancer specific immune responses or by modifying native immune processes and clinical response, patterns have shown to extend beyond those of cytotoxic agents (76). RECIST or WHO criteria, designed to detect early effects of cytotoxic agents may not provide a complete assessment when using immunotherapeutic agents. Wolchok *et al.* described four distinct patterns of treatment response after ipilimumab treatment for metastatic melanoma (76) which were all associated with favourable survival: (I) the lesion volume decreased from the beginning; (II) there was a “stable disease” with slow, steady decline in total tumor volume; (III) response occurred after an initial increase in total

tumor volume or (IV) the total tumor burden decreased but new lesions appeared. The authors stated that these response criteria will need further prospective evaluations and particularly their association with overall survival will have to be evaluated (76).

Stereotactic radiosurgery (SRS) is an already established effective technique for local treatment of brain metastases and assessing treatment response after SRS is important to plan further therapeutic steps. The most studied and robust neuroimaging modality in this context is DW-MRI. Studies evaluating ADC and DW-MRI values before and after radiation treatment showed that DW-MRI values decrease and ADC values increase in responsive patients (77,78). Lee *et al.* showed that the sensitivity of a decrease in the DW-MRI ratio in making an early prediction of tumor control was 83.9% and the specificity was 88.5%. When using the initial ADC values of metastases to predict tumor response, sensitivity and specificity were 85.5 and 72.7%, respectively (78). Using perfusions MRI Jakubovic *et al.* (79) showed that early assessment of CBV and vascular permeability (ktrans) may serve as MRI biomarkers of radiation response or progression for brain metastases, as in 44 patients CBV as well as ktrans at 1 week after treatment could differentiate between a responder and a non-responder to radiation treatment (79). In another study (n=26) an increase in ktrans of 15% showed a sensitivity of 78% and a specificity of 85% for the prediction of progression at 4 weeks after SRS treatment (80). Even the pretherapeutic regional CBV (81) proved to be highly sensitive and specific for treatment outcome at the 6-week follow-up and a decrease of the regional CBV value at 6 weeks helped predict the treatment outcome with a sensitivity of more than 90% (81).

Discriminating radiation necrosis from recurrent tumor

Following treatment with SRS, however, radiologists are also sometimes confronted and confused by radiation-induced injuries, including pseudo-progression and radiation necrosis. Both conditions present with contrast enhancement on T1 weighted MR images and the pattern of abnormal enhancement closely mimics that of a recurrent brain metastasis. So, classifying newly developed abnormal enhancing lesions in follow-up of treated brain metastasis is one of the key goals in neuro-oncologic imaging (82). Again, functional MRI and PET help to detect hemodynamic, metabolic, and cellular alterations.

Small studies in perfusion MRI using CBV analysis showed the potential to differentiate between radiation necrosis and tumor recurrence with good sensitivity and specificity (83,84).

Nuclear medicine techniques play a major role answering this critical question. As far as the applied tracer is concerned, ^{18}F -FDG was shown to be not sensitive enough to differentiate vital brain metastases from unspecific non-tumor changes related to therapy (85). With the amino acid PET tracer ^{11}C -MET (^{11}C -Methionine), however, it could be shown that in 51 patients with brain metastases and 26 with glioma, tumor to lesion uptake ratios in patients with recurrent metastases/glioma after radiation treatment was higher than in radiation necrosis (86). Using two amino acid tracers (^{18}F -FET and ^{11}C -MET) Grosu *et al.* (87) was able to differentiate tumor and treatment-related changes with a sensitivity of 91% and a specificity of 100% (87). Galldiks *et al.* (88) showed that dynamic ^{18}F -FET PET (consisting of image acquisition up to 50 minutes after radiopharmaceutical intravenous injection and calculation of time activity curves, as well as calculation of maximum and mean tumor-to-brain ratios of standard ^{18}F -FET uptake) was able to differentiate local recurrent brain metastases and radiation necrosis with a high diagnostic accuracy. The potential role of nuclear medicine is further underlined by a study following SRS in 42 patients with 50 brain metastases using ^{18}F -DOPA PET, where this modality proved to accurately differentiate radiation necrosis from progressive disease with a sensitivity of 90% and a specificity of 92.3%. In this study, ^{18}F -DOPA PET also seemed to perform better than perfusion MRI with a sensitivity of 86.7% and a specificity of 68.2% (89).

Prediction of prognosis

Several risk stratification scores have been developed to guide therapeutic decisions and to predict patient survival. The three established scores are the Recursive Partitioning Analysis (RPA), the Graded Prognostic Assessment (GPA) and Diagnosis Specific Graded Prognostic Assessment (DS-GPA) (3,90,91). Variables on neuroimaging with the exception of the number of brain metastases, are currently not considered for prognostic risk stratification. However, efforts are being made to include neuroimaging parameters into these established scores (92,93). The prognostic value of the extent of the peritumoral edema in 118 patients operated on for single brain metastases was analyzed by Spanberger and colleagues. They found a significant correlation with a small brain edema with an invasive tumor

growth pattern, a low neo-angiogenic activity and a low expression of HIF1 α . These findings were associated with a shorter overall survival (93). Evidence from other solid organ cancers and metastases suggest that DW-MRI may be used as a biomarker of prognosis and treatment response. The same study group investigated DW-MRI parameters pre-operatively in single brain metastases and found that high DW-MRI hyperintensity correlated significantly with a high amount of interstitial reticulin deposition and this was again associated with worse survival (92). Similarly, Zakaria *et al.* showed that pre-operative DW-MRI characteristics of cerebral metastases and their peritumoral region in 76 patients are related to patient outcomes (94).

New imaging tools and contrasts

Novel MRI contrast based on the chemical exchange saturation transfer (CEST) proved to be relevant in brain tumor imaging (95). CEST imaging visualizes endogenous mobile proteins, metabolites and peptides and their tissue specific concentrations, making it to an attractive technology with the potential for frequency selective molecular imaging (96). Currently, no CEST studies on secondary brain tumors are available. It has already been shown, however, that CEST Imaging at 7 Tesla provides additional information on the structure of peritumoral hyperintensities in glioblastoma and displays isolated high intensity regions within the contrast enhanced tumor that cannot be detected on contrast enhanced T1 weighted or T2-weighted images (97).

Summary

With the development of new imaging techniques, the potential to investigate the molecular, cellular and structural components of the tumor microenvironment *in situ* has increased substantially. In the light of new treatment strategies, it will become increasingly important to visualize the expression of molecules and cell motion as well as to enhance the technical possibility to calculate cellularity, vessel permeability, vascular perfusion, metabolic and physiological changes, apoptosis and inflammation—prior to and during the course of therapy. Currently, major evidence suggests that quantitative neuroimaging parameters from Perfusion MRI, DW-MRI or MRS in the peritumoral region may provide supplementary information to differentiating primary from secondary brain tumors and that amino acid PET is useful in discriminating radiation

necrosis from recurrent tumor. A multimodal approach combining parameters derived from each of the advanced imaging techniques is likely to improve sensitivity and specificity in diagnostic and response assessment. To achieve high diagnostic accuracy however, large multicenter studies will have to be carried out and imaging protocols including post-processing procedures have to be standardized.

Acknowledgements

The authors deeply thank Prof. Dr. Günther Stockhammer for critical review and for suggesting helpful improvements to the manuscript.

Disclosure: The authors declare no conflict of interest.

References

1. Lin NU, Amiri-Kordestani L, Palmieri D, et al. CNS metastases in breast cancer: old challenge, new frontiers. *Clin Cancer Res* 2013;19:6404-18.
2. Fox BD, Cheung VJ, Patel AJ, et al. Epidemiology of metastatic brain tumors. *Neurosurg Clin N Am* 2011;22:1-6, v.
3. Sperduto PW, Kased N, Roberge D, et al. Summary report on the graded prognostic assessment: an accurate and facile diagnosis-specific tool to estimate survival for patients with brain metastases. *J Clin Oncol* 2012;30:419-25.
4. Chen AM, Jahan TM, Jablons DM, et al. Risk of cerebral metastases and neurological death after pathological complete response to neoadjuvant therapy for locally advanced nonsmall-cell lung cancer: clinical implications for the subsequent management of the brain. *Cancer* 2007;109:1668-75.
5. Hutterer M, Nowosielski M, Putzer D, et al. [18F]-fluoro-ethyl-L-tyrosine PET: a valuable diagnostic tool in neuro-oncology, but not all that glitters is glioma. *Neuro Oncol* 2013;15:341-51.
6. Suchorska B, Tonn JC, Jansen NL. PET imaging for brain tumor diagnostics. *Curr Opin Neurol* 2014;27:683-8.
7. Cufer T, Knez L. Update on systemic therapy of advanced non-small-cell lung cancer. *Expert Rev Anticancer Ther* 2014;14:1189-203.
8. Andrews MC, Woods K, Cebon J, et al. Evolving role of tumor antigens for future melanoma therapies. *Future Oncol* 2014;10:1457-68.
9. Jackson SE, Chester JD. Personalised cancer medicine. *Int J Cancer* 2015;137:262-6.
10. van Kruchten M, de Vries EG, Brown M, et al. PET

- imaging of oestrogen receptors in patients with breast cancer. *Lancet Oncol* 2013;14:e465-75.
11. Dhermain FG, Hau P, Lanfermann H, et al. Advanced MRI and PET imaging for assessment of treatment response in patients with gliomas. *Lancet Neurol* 2010;9:906-20.
 12. Le Bihan D, Breton E, Lallemand D, et al. Separation of diffusion and perfusion in intravoxel incoherent motion MR imaging. *Radiology* 1988;168:497-505.
 13. Padhani AR, Liu G, Koh DM, et al. Diffusion-weighted magnetic resonance imaging as a cancer biomarker: consensus and recommendations. *Neoplasia* 2009;11:102-25.
 14. Fink KR, Fink JR. Imaging of brain metastases. *Surg Neurol Int* 2013;4:S209-19.
 15. Thompson G, Mills SJ, Stivaros SM, et al. Imaging of brain tumors: perfusion/permeability Neuroimaging Clin N Am 2010;20:337-53.
 16. Jackson A, O'Connor J, Thompson G, et al. Magnetic resonance perfusion imaging in neuro-oncology. *Cancer Imaging* 2008;8:186-99.
 17. van der Graaf M. In vivo magnetic resonance spectroscopy: basic methodology and clinical applications. *Eur Biophys J* 2010;39:527-40.
 18. Bénard F, Romsa J, Hustinx R. Imaging gliomas with positron emission tomography and single-photon emission computed tomography. *Semin Nucl Med* 2003;33:148-62.
 19. Palumbo B. Brain tumour recurrence: brain single-photon emission computerized tomography, PET and proton magnetic resonance spectroscopy. *Nucl Med Commun* 2008;29:730-5.
 20. Kickingreder P, Dorn F, Blau T, et al. Differentiation of local tumor recurrence from radiation-induced changes after stereotactic radiosurgery for treatment of brain metastasis: case report and review of the literature. *Radiat Oncol* 2013;8:52.
 21. Langen KJ, Hamacher K, Weckesser M, et al. O-(2-[18F] fluoroethyl)-L-tyrosine: uptake mechanisms and clinical applications. *Nucl Med Biol* 2006;33:287-94.
 22. Galldiks N, Langen KJ. 2014. Applications of PET imaging of neurological tumors with radiolabeled amino acids. Available online: <http://scicurve.com/paper/25517079>
 23. Jager PL, Vaalburg W, Pruijm J, et al. Radiolabeled amino acids: basic aspects and clinical applications in oncology. *J Nucl Med* 2001;42:432-45.
 24. Stockhammer F, Plotkin M, Amthauer H, et al. Correlation of F-18-fluoro-ethyl-tyrosin uptake with vascular and cell density in non-contrast-enhancing gliomas. *J Neurooncol* 2008;88:205-10.
 25. Ullrich R, Backes H, Li H, et al. Glioma proliferation as assessed by 3'-fluoro-3'-deoxy-L-thymidine positron emission tomography in patients with newly diagnosed high-grade glioma. *Clin Cancer Res* 2008;14:2049-55.
 26. Soffietti R, Cornu P, Delattre JY, et al. EFNS Guidelines on diagnosis and treatment of brain metastases: report of an EFNS Task Force. *Eur J Neurol* 2006;13:674-81.
 27. Eberhardt WE, De Ruyscher D, Weder W, et al. 2nd ESMO Consensus Conference in Lung Cancer: locally-advanced stage III non-small-cell lung cancer (NSCLC). *Ann Oncol* 2015. [Epub ahead of print].
 28. Cardoso F, Costa A, Norton L, et al. ESO-ESMO 2nd international consensus guidelines for advanced breast cancer (ABC2) dagger. *Ann Oncol* 2014;25:1871-88.
 29. Dummer R, Hauschild A, Guggenheim M, et al. Cutaneous melanoma: ESMO Clinical Practice Guidelines for diagnosis, treatment and follow-up. *Ann Oncol* 2012;23 Suppl 7:vii86-91.
 30. O'Dowd EL, Kumaran M, Anwar S, et al. Brain metastases following radical surgical treatment of non-small cell lung cancer: is preoperative brain imaging important? *Lung Cancer* 2014;86:185-9.
 31. Kung BT, Auyong TK, Tong CM. Prevalence of detecting unknown cerebral metastases in fluorodeoxyglucose positron emission tomography/computed tomography and its potential clinical impact. *World J Nucl Med* 2014;13:108-11.
 32. Schellinger PD, Meinck HM, Thron A. Diagnostic accuracy of MRI compared to CCT in patients with brain metastases. *J Neurooncol* 1999;44:275-81.
 33. Sze G, Johnson C, Kawamura Y, et al. Comparison of single- and triple-dose contrast material in the MR screening of brain metastases. *AJNR Am J Neuroradiol* 1998;19:821-8.
 34. Mills SJ, Thompson G, Jackson A. Advanced magnetic resonance imaging biomarkers of cerebral metastases. *Cancer Imaging* 2012;12:245-52.
 35. Breckwoldt M, Bendszus M. Cerebral MR imaging of malignant melanoma. *Radiologe* 2015;55:113-9.
 36. Desprechins B, Stadnik T, Koerts G, et al. Use of diffusion-weighted MR imaging in differential diagnosis between intracerebral necrotic tumors and cerebral abscesses. *AJNR Am J Neuroradiol* 1999;20:1252-7.
 37. Hartmann M, Jansen O, Heiland S, et al. Restricted diffusion within ring enhancement is not pathognomonic for brain abscess. *AJNR Am J Neuroradiol*

- 2001;22:1738-42.
38. Kim YJ, Chang KH, Song IC, et al. Brain abscess and necrotic or cystic brain tumor: discrimination with signal intensity on diffusion-weighted MR imaging. *AJR Am J Roentgenol* 1998;171:1487-90.
 39. Duyugulu G, Ovali GY, Calli C, et al. Intracerebral metastasis showing restricted diffusion: correlation with histopathologic findings. *Eur J Radiol* 2010;74:117-20.
 40. Lu S, Ahn D, Johnson G, et al. Peritumoral diffusion tensor imaging of high-grade gliomas and metastatic brain tumors. *AJNR Am J Neuroradiol* 2003;24:937-41.
 41. Pavlisa G, Rados M, Pavlisa G, et al. The differences of water diffusion between brain tissue infiltrated by tumor and peritumoral vasogenic edema. *Clin Imaging* 2009;33:96-101.
 42. Bulakbasi N, Guvenc I, Onguru O, et al. The added value of the apparent diffusion coefficient calculation to magnetic resonance imaging in the differentiation and grading of malignant brain tumors. *J Comput Assist Tomogr* 2004;28:735-46.
 43. Yamasaki F, Kurisu K, Satoh K, et al. Apparent diffusion coefficient of human brain tumors at MR imaging. *Radiology* 2005;235:985-91.
 44. Berghoff AS, Rajky O, Winkler F, et al. Invasion patterns in brain metastases of solid cancers. *Neuro Oncol* 2013;15:1664-72.
 45. Bulakbasi N, Kocaoglu M, Farzaliyev A, et al. Assessment of diagnostic accuracy of perfusion MR imaging in primary and metastatic solitary malignant brain tumors. *AJNR Am J Neuroradiol* 2005;26:2187-99.
 46. Law M, Cha S, Knopp EA, et al. High-grade gliomas and solitary metastases: differentiation by using perfusion and proton spectroscopic MR imaging. *Radiology* 2002;222:715-21.
 47. Young GS, Setayesh K. Spin-echo echo-planar perfusion MR imaging in the differential diagnosis of solitary enhancing brain lesions: distinguishing solitary metastases from primary glioma. *AJNR Am J Neuroradiol* 2009;30:575-7.
 48. Calli C, Kitis O, Yunten N, et al. Perfusion and diffusion MR imaging in enhancing malignant cerebral tumors. *Eur J Radiol* 2006;58:394-403.
 49. Toh CH, Wei KC, Chang CN, et al. Differentiation of brain abscesses from glioblastomas and metastatic brain tumors: comparisons of diagnostic performance of dynamic susceptibility contrast-enhanced perfusion MR imaging before and after mathematic contrast leakage correction. *PLoS One* 2014;9:e109172.
 50. Chiang IC, Kuo YT, Lu CY, et al. Distinction between high-grade gliomas and solitary metastases using peritumoral 3-T magnetic resonance spectroscopy, diffusion, and perfusion imagings. *Neuroradiology* 2004;46:619-27.
 51. Server A, Josefsen R, Kulle B, et al. Proton magnetic resonance spectroscopy in the distinction of high-grade cerebral gliomas from single metastatic brain tumors. *Acta Radiol* 2010;51:316-25.
 52. Huang BY, Kwock L, Castillo M, et al. Association of choline levels and tumor perfusion in brain metastases assessed with proton MR spectroscopy and dynamic susceptibility contrast-enhanced perfusion weighted MRI. *Technol Cancer Res Treat* 2010;9:327-37.
 53. Radbruch A, Graf M, Kramp L, et al. Differentiation of brain metastases by percentage-wise quantification of intratumoral-susceptibility-signals at 3 Tesla. *Eur J Radiol* 2012;81:4064-8.
 54. Ding Y, Xing Z, Liu B, et al. Differentiation of primary central nervous system lymphoma from high-grade glioma and brain metastases using susceptibility-weighted imaging. *Brain Behav* 2014;4:841-9.
 55. Feng W, Zhang P, Zheng X, et al. Neuroimaging and clinical characteristics of brain metastases from esophageal carcinoma in Chinese patients. *J Cancer Res Ther* 2014;10 Suppl:296-303.
 56. Yeh RH, Yu JC, Chu CH, et al. Distinct MR Imaging Features of Triple-Negative Breast Cancer with Brain Metastasis. *J Neuroimaging* 2015;25:474-81.
 57. Momose T, Nariai T, Kawabe T, et al. Clinical benefit of ¹¹C methionine PET imaging as a planning modality for radiosurgery of previously irradiated recurrent brain metastases. *Clin Nucl Med* 2014;39:939-43.
 58. Zakaria R, Jenkinson MD. Using ADC Maps with Structural Scans to Improve Intraoperative Biopsy Specimens in Brain Metastases. *Neuroradiol J* 2014;27:422-4.
 59. Mardor Y, Roth Y, Ochershvilli A, et al. Pretreatment prediction of brain tumors' response to radiation therapy using high b-value diffusion-weighted MRI. *Neoplasia* 2004;6:136-42.
 60. Therasse P, Arbuck SG, Eisenhauer EA, et al. New guidelines to evaluate the response to treatment in solid tumors. European Organization for Research and Treatment of Cancer, National Cancer Institute of the United States, National Cancer Institute of Canada. *J Natl Cancer Inst* 2000;92:205-16.
 61. Lin NU, Lee EQ, Aoyama H. Challenges relating to solid

- tumour brain metastases in clinical trials, part 1: patient population, response, and progression. A report from the RANO group. *Lancet Oncol* 2013;14:e396-406.
62. Wen PY, Macdonald DR, Reardon DA, et al. Updated response assessment criteria for high-grade gliomas: response assessment in neuro-oncology working group. *J Clin Oncol* 2010;28:1963-72.
 63. Shankar LK, Hoffman JM, Bacharach S, et al. Consensus recommendations for the use of 18F-FDG PET as an indicator of therapeutic response in patients in National Cancer Institute Trials. *J Nucl Med* 2006;47:1059-66.
 64. Dijkers EC, Oude Munnink TH, Kosterink JG, et al. Biodistribution of 89Zr-trastuzumab and PET imaging of HER2-positive lesions in patients with metastatic breast cancer. *Clin Pharmacol Ther* 2010;87:586-92.
 65. Gaykema SB, Brouwers AH, Lub-de Hooge MN, et al. 89Zr-bevacizumab PET imaging in primary breast cancer. *J Nucl Med* 2013;54:1014-8.
 66. Vredenburgh JJ, Desjardins A, Herndon JE 2nd, et al. Bevacizumab plus irinotecan in recurrent glioblastoma multiforme. *J Clin Oncol* 2007;25:4722-9.
 67. Brandsma D, van den Bent MJ. Pseudoprogression and pseudoresponse in the treatment of gliomas. *Curr Opin Neurol* 2009;22:633-8.
 68. van den Bent MJ, Vogelbaum MA, Wen PY, et al. End point assessment in gliomas: novel treatments limit usefulness of classical Macdonald's Criteria. *J Clin Oncol* 2009;27:2905-8.
 69. Nowosielski M, Recheis W, Goebel G, et al. ADC histograms predict response to anti-angiogenic therapy in patients with recurrent high-grade glioma. *Neuroradiology* 2011;53:291-302.
 70. Pope WB, Kim HJ, Huo J, et al. Recurrent glioblastoma multiforme: ADC histogram analysis predicts response to bevacizumab treatment. *Radiology* 2009;252:182-9.
 71. Sorensen AG, Batchelor TT, Zhang WT, et al. A "vascular normalization index" as potential mechanistic biomarker to predict survival after a single dose of cediranib in recurrent glioblastoma patients. *Cancer Res* 2009;69:5296-300.
 72. Kickingeder P, Wiestler B, Burth S, et al. Relative cerebral blood volume is a potential predictive imaging biomarker of bevacizumab efficacy in recurrent glioblastoma. *Neuro Oncol* 2015. [Epub ahead of print].
 73. Hattingen E, Jurcoane A, Bähr O, et al. Bevacizumab impairs oxidative energy metabolism and shows antitumoral effects in recurrent glioblastomas: a 31P/1H MRSI and quantitative magnetic resonance imaging study. *Neuro Oncol* 2011;13:1349-63.
 74. Hattingen E, Jurcoane A, Daneshvar K, et al. Quantitative T2 mapping of recurrent glioblastoma under bevacizumab improves monitoring for non-enhancing tumor progression and predicts overall survival. *Neuro Oncol* 2013;15:1395-404.
 75. Ellingson BM, Kim HJ, Woodworth DC, et al. Recurrent glioblastoma treated with bevacizumab: contrast-enhanced T1-weighted subtraction maps improve tumor delineation and aid prediction of survival in a multicenter clinical trial. *Radiology* 2014;271:200-10.
 76. Wolchok JD, Hoos A, O'Day S, et al. Guidelines for the evaluation of immune therapy activity in solid tumors: immune-related response criteria. *Clin Cancer Res* 2009;15:7412-20.
 77. Mardor Y, Pfeffer R, Spiegelmann R, et al. Early detection of response to radiation therapy in patients with brain malignancies using conventional and high b-value diffusion-weighted magnetic resonance imaging. *J Clin Oncol* 2003;21:1094-100.
 78. Lee CC, Wintermark M, Xu Z, et al. Application of diffusion-weighted magnetic resonance imaging to predict the intracranial metastatic tumor response to gamma knife radiosurgery. *J Neurooncol* 2014;118:351-61.
 79. Jakubovic R, Sahgal A, Soliman H, et al. Magnetic resonance imaging-based tumour perfusion parameters are biomarkers predicting response after radiation to brain metastases. *Clin Oncol (R Coll Radiol)* 2014;26:704-12.
 80. Almeida-Freitas DB, Pinho MC, Otaduy MC, et al. Assessment of irradiated brain metastases using dynamic contrast-enhanced magnetic resonance imaging. *Neuroradiology* 2014;56:437-43.
 81. Essig M, Waschkes M, Wenz F, et al. Assessment of brain metastases with dynamic susceptibility-weighted contrast-enhanced MR imaging: initial results. *Radiology* 2003;228:193-9.
 82. Kang TW, Kim ST, Byun HS, et al. Morphological and functional MRI, MRS, perfusion and diffusion changes after radiosurgery of brain metastasis. *Eur J Radiol* 2009;72:370-80.
 83. Hoefnagels FW, Lagerwaard FJ, Sanchez E, et al. Radiological progression of cerebral metastases after radiosurgery: assessment of perfusion MRI for differentiating between necrosis and recurrence. *J Neurol* 2009;256:878-87.
 84. Mitsuya K, Nakasu Y, Horiguchi S, et al. Perfusion weighted magnetic resonance imaging to distinguish the recurrence of metastatic brain tumors from radiation necrosis after stereotactic radiosurgery. *J Neurooncol*

- 2010;99:81-8.
85. Krüger S, Mottaghy FM, Buck AK, et al. Brain metastasis in lung cancer. Comparison of cerebral MRI and 18F-FDG-PET/CT for diagnosis in the initial staging. *Nuklearmedizin* 2011;50:101-6.
 86. Terakawa Y, Tsuyuguchi N, Iwai Y, et al. Diagnostic accuracy of 11C-methionine PET for differentiation of recurrent brain tumors from radiation necrosis after radiotherapy. *J Nucl Med* 2008;49:694-9.
 87. Grosu AL, Astner ST, Riedel E, et al. An interindividual comparison of O-(2-[18F]fluoroethyl)-L-tyrosine (FET)- and L-[methyl-11C]methionine (MET)-PET in patients with brain gliomas and metastases. *Int J Radiat Oncol Biol Phys* 2011;81:1049-58.
 88. Galldiks N, Stoffels G, Filss CP, et al. Role of O-(2-(18)F-fluoroethyl)-L-tyrosine PET for differentiation of local recurrent brain metastasis from radiation necrosis. *J Nucl Med* 2012;53:1367-74.
 89. Cicone F, Minniti G, Romano A, et al. Accuracy of F-DOPA PET and perfusion-MRI for differentiating radionecrotic from progressive brain metastases after radiosurgery. *Eur J Nucl Med Mol Imaging* 2015;42:103-11.
 90. Sperduto PW, Berkey B, Gaspar LE, et al. A new prognostic index and comparison to three other indices for patients with brain metastases: an analysis of 1,960 patients in the RTOG database. *Int J Radiat Oncol Biol Phys* 2008;70:510-4.
 91. Gaspar L, Scott C, Rotman M, et al. Recursive partitioning analysis (RPA) of prognostic factors in three Radiation Therapy Oncology Group (RTOG) brain metastases trials. *Int J Radiat Oncol Biol Phys* 1997;37:745-51.
 92. Berghoff AS, Spanberger T, Ilhan-Mutlu A, et al. Preoperative diffusion-weighted imaging of single brain metastases correlates with patient survival times. *PLoS One* 2013;8:e55464.
 93. Spanberger T, Berghoff AS, Dinhof C, et al. Extent of peritumoral brain edema correlates with prognosis, tumoral growth pattern, HIF1a expression and angiogenic activity in patients with single brain metastases. *Clin Exp Metastasis* 2013;30:357-68.
 94. Zakaria R, Das K, Radon M, et al. Diffusion-weighted MRI characteristics of the cerebral metastasis to brain boundary predicts patient outcomes. *BMC Med Imaging* 2014;14:26.
 95. Zaiss M, Windschuh J, Paech D, et al. Relaxation-compensated CEST-MRI of the human brain at 7T: Unbiased insight into NOE and amide signal changes in human glioblastoma. *Neuroimage* 2015;112:180-8.
 96. Liu G, Song X, Chan KW, et al. Nuts and bolts of chemical exchange saturation transfer MRI. *NMR Biomed* 2013;26:810-28.
 97. Paech D, Zaiss M, Meissner JE, et al. Nuclear overhauser enhancement mediated chemical exchange saturation transfer imaging at 7 Tesla in glioblastoma patients. *PLoS One* 2014;9:e104181.

Cite this article as: Nowosielski M, Radbruch A. The emerging role of advanced neuroimaging techniques for brain metastases. *Chin Clin Oncol* 2015;4(2):23. doi: 10.3978/j.issn.2304-3865.2015.05.04